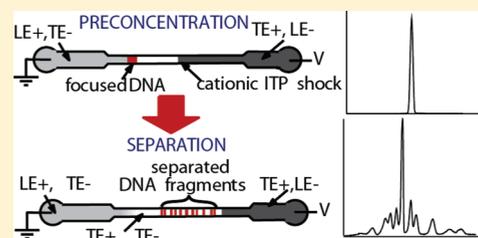# Coupled Isotachophoretic Preconcentration and Electrophoretic Separation Using Bidirectional Isotachophoresis

Supreet S. Bahga, Robert D. Chambers, and Juan G. Santiago*

Department of Mechanical Engineering, Stanford University, California 94305, United States

S *Supporting Information*

ABSTRACT: We present a novel technique for coupling isotachophoretic preconcentration and electrophoretic separation using bidirectional isotachophoresis (ITP). Bidirectional ITP simultaneously sets up sharp ITP interfaces between relatively high- and low-mobility cations and high- and low-mobility anions. These two interfaces can migrate toward each other and be described as ion concentration shock waves. We here demonstrate a bidirectional ITP process in which we use the interaction of these anionic and cationic ITP shock waves to trigger a transformation from ITP preconcentration to electrophoretic separation. We use anionic ITP to focus anionic sample species prior to shock interaction. The interaction of the counter-propagating anionic and cationic ITP shocks then changes the local pH (and ionic strength) of the focused analyte zones. Under this new condition, the analytes no longer focus and begin to separate electrophoretically. The method provides faster and much less dispersive transition from ITP preconcentration to electrophoretic separation compared with traditional (unidirectional) transient ITP. It eliminates the need for intermediate steps between focusing and separation, such as manual buffer exchanges. We illustrate the technique with numerical simulations of species transport equations. We have validated our simulations with experimental visualization of bidirectional ITP zones. We then show the effectiveness of the technique by coupling ITP preconcentration and high-resolution separation of a 1 kbp DNA ladder via shock interaction in bidirectional ITP.

Isotachophoresis (ITP) is a preconcentration and separation technique that leverages electrolytes with different electrophoretic mobility to focus (and in some cases, separate) ionic analytes into distinct zones. In ITP, analytes simultaneously focus and separate between high effective mobility leading electrolyte (LE) ions and low effective mobility trailing electrolyte (TE) ions.[1,2] The balance of electromigration and diffusion at the zone boundaries in ITP results in sharp moving boundaries, which can be described as ion concentration shock waves.[3−5] Shock waves due to nonlinear electromigration flux in electrophoresis and ITP have been shown theoretically by Zhukov[3] and Moore[4] and experimentally by, for example, Ermakov et al.[10] and Thormann.[11]

Typically, ITP experiments are performed separately for focusing anions or cations in anionic and cationic ITP, respectively; however, anionic and cationic ITP can also be performed simultaneously in a single channel.[12,13] The latter approach, called bidirectional ITP, is characterized by anionic and cationic ITP shock waves propagating in opposite directions. Depending on the initial conditions, shocks in bidirectional ITP can be made to propagate either toward or away from each other.[13,14] Kohlrausch[13,15] first proposed the idea of bidirectional ITP with diverging shocks, characterized by anionic and cationic ITP shocks moving apart. Since then, it has been used to simultaneously separate cationic and anionic components of samples.[12,16,17] Oshurkova and Ivanova[18] first demonstrated bidirectional ITP in so-called "converging" mode in which cationic and anionic shocks approach each other. They used bidirectional ITP to measure the concentration of a binary electrolyte solution. The

anions and cations of this binary electrolyte solution formed the respective LE ions of the simultaneous anionic and cationic ITP processes.[18,19] Since the Oshurkova and Ivanova study, we know of no further work on the study of converging ITP shocks. To our knowledge, all bidirectional ITP studies with converging shocks are limited to the case that the system is analyzed prior to the interaction of anionic and cationic shock waves.[18,19] For example, the Oshurkova and Ivanova[18] quantified the concentration of the LE by analyzing the rate of convergence of the two shocks. However, they do not discuss or present analysis of ion concentrations or shock propagation velocities after the interaction of cationic and anionic ITP shocks. We know of no previous work studying the effect of shock interactions on different zones in bidirectional ITP.

We view shock interaction in bidirectional ITP as an important process because it can lead to fundamental modification of the electrophoretic conditions. For example, shock interaction can initiate changes in counterion species, concentration of co-ion species, local pH (e.g., changing effective mobility), and species zone order. We here submit that shock interactions in bidirectional ITP can be used to initiate either modified ITP modes or electrophoresis modes. In the current work, we establish a bidirectional ITP experiment in which shock interaction triggers a transformation from ITP preconcentration to

electrophoretic separation. Traditional ITP buffer systems use only two co-ionic species (leading and trailing) and a single counterionic species. Here, our bidirectional experiments require four species (i.e., two oppositely charged pairs of leading and trailing ions) which we term LE+, LE−, TE+, and TE−. Here, LE and TE again denote the leading and the trailing electrolyte ions, respectively, and + and − correspond to cations and anions, respectively. We explore the case of anionic analytes initially focused between TE− and LE−. Before the anionic and cationic ITP shocks meet, the counterion of the focused analyte zones is LE+. After these shocks meet, TE+ replaces LE+ as the counterion for analyte zones. This changes the pH such that ITP focusing conditions for analyte ions no longer hold, and consequently, analytes begin to separate electrophoretically. The method negates the need for deactivating power during the experiment or manual buffer exchanges as in typical transient ITP (t-ITP) experiments.[20−22]

We begin by describing the principle of coupling ITP pre-concentration and electrophoretic separation using bidirectional ITP with converging anionic and cationic ITP shock waves. We discuss choices of electrolyte chemistries appropriate for coupling ITP focusing and electrophoretic separation. We then present simulations to illustrate the technique and verify our choice of electrolyte chemistry. We confirm these simulations by experimental visualization of interacting anionic and cationic ITP shocks. Using simulations, we then compare the separation resolution of bidirectional ITP and t-ITP. Finally, using our technique, we experimentally demonstrate coupled ITP pre-concentration and high-resolution separation of a 1 kbp ds-DNA ladder.

■ THEORY

Concept of Initiating Electrophoresis via ITP Shock Interaction. In ITP, analyte ions focus only if their charge has the same sign as respective LE and TE ions. Two other requirements for focusing analyte ions are that analyte ions should have higher effective mobility (μ) than TE ions in both TE and analyte zones,

$$|\mu_{a,T}| > |\mu_{te,T}|, \quad |\mu_{a,A}| > |\mu_{te,A}| \tag{1}$$

and that the effective mobility of analyte ions should be smaller than that of LE ions in both LE and analyte zones,[23]

$$|\mu_{a,L}| < |\mu_{le,L}|, \quad |\mu_{a,A}| < |\mu_{le,A}| \tag{2}$$

In our notation, the first (lower case) subscript indicates the chemical species and the second (capital) subscript indicates the zone of interest. Subscripts a, te, le therefore denote analyte, TE, and LE ions, respectively, and subscripts A, T, L denote analyte, TE, and LE zones.

Whether and when the ITP focusing conditions given by eqs 1 and 2 are valid depends strongly on local conditions, because effective mobility is a strong function of pH[24] and a weaker function of ionic strength.[25,26] For example, the effective mobility of a weak acid analyte increases monotonically with increasing pH and saturates at the lowest (negative) valence. Conversely, the effective mobility of a weak base decreases with increasing pH may saturate at the highest valence. In this work, we will consider only singly ionized ions so that the aforementioned saturation values are the fully ionized mobilities of the +1 cation and −1 anion, respectively. See Persat et al.[24] for a review of the interplay
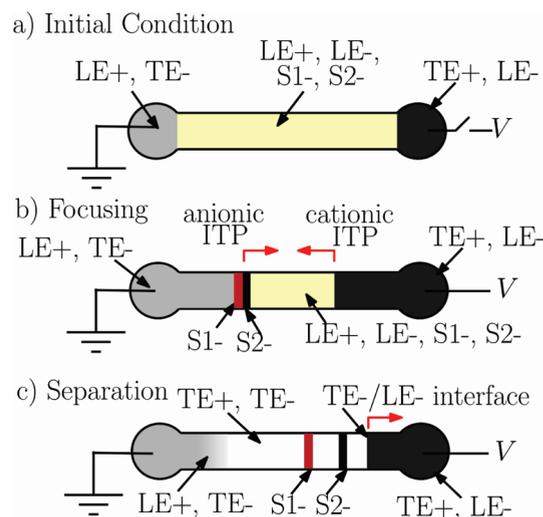
Figure 1. Schematic illustrating focusing and separation of analytes using bidirectional ITP. (a) The channel is initially filled with a mixture of LE+, LE−, and analytes S1− and S2−. The reservoir on the left is filled with the LE+/ TE− mixture, and the reservoir on the right is filled with the TE+/LE− mixture. Buffers are chosen such that LE+ is a cation of a weak base with high mobility and TE+ is a cation of a strong base with low mobility. Furthermore, LE− is an anion of a strong acid with high mobility, and TE− is an anion of weak acid with low mobility. (b) When voltage is applied, the anionic analytes focus between LE− and TE−. The focused analyte zones propagate toward the right. Simultaneously, a leftward-propagating cationic ITP shock forms between LE+ and TE+ zones. Because TE+ is a stronger base than LE+, TE+ raises the pH behind the LE+/TE+ shock. (c) When the LE+/TE+ shock washes over the focused anionic analytes, it similarly raises the pH of anionic ITP zones. The increase in pH of anionic ITP zones increases the local value of the effective mobility of TE− (an anion of a weak acid). Thereafter, TE− ions overtake the focused analyte ions, breaking the ITP focusing conditions for S1− and S2−. Consequently, the anionic analytes S1− and S2− cease focusing and commence electrophoretic separation.

between electromigration and buffer chemistry, particularly effective mobility versus pH.

In this work, we use bidirectional ITP with converging shocks to quickly and precisely alter the pH of migrating ITP zones so that analytes isotachophoretically focus before the shock interaction and electrophoretically separate thereafter. Figure 1 shows a schematic of our technique. We fill a simple, straight channel with a mixture of LE+, LE−, and anionic analytes (S1− and S2−), as shown in Figure 1a. LE+ and LE− serve as leading electrolyte ions for cationic and anionic ITP, respectively. We fill the reservoir on the left with a mixture of TE− and LE+ (LE+ acts as the counterion). Similarly, we fill the reservoir on the right with TE+ and LE−. For anionic ITP, we choose LE−, TE−, and a background counterion (LE+) such that ITP focusing conditions (given by eqs 1 and 2) hold for analytes S1− and S2− prior to the shock interaction. As shown in Figure 1b, when voltage is applied across the channel, S1− and S2− focus between the LE− and the TE− zones. The anionic ITP (LE−/TE− interface) shock propagates toward the right, and the cationic ITP shock (LE+/TE+ interface) propagates toward the left. Subsequently, the shocks meet and interact. The LE+/TE+ shock sweeps over the focused anionic analytes, replacing the local LE+ counterions with TE+ ions. In this newly created region where TE+ ions replaced the LE+ ions, the pH and effective mobilities

of the buffer and analyte ions change. To initiate electrophoretic separation, we choose the conditions such that the effective mobility of TE− in the newly created zone is larger than the effective mobilities of S1− and S2−. This causes TE− ions to overtake and pass the analyte zones. Thereafter, S1− and S2− separate, as in capillary zone electrophoresis (Figure 1c).

In our bidirectional ITP experiments, the cationic ITP interface plays no role in the initial ITP focusing of analytes at the anionic ITP interface. The purpose of cationic ITP is to initiate electrophoretic separation of these analytes upon interaction of the anionic and cationic ITP shocks. Therefore, we note that our technique differs markedly from unidirectional transient ITP (t-ITP)[20−22] wherein LE ions are injected behind focused anionic samples to initiate separation.

There are several choices to be made in designing ITP shock interactions that initiate electrophoretic separation. We here focus our discussion on choosing electrolytes (LE+, LE−, TE+, and TE−) to preconcentrate and separate strongly ionized analytes, such as nucleic acids. However, we note that our technique is also applicable to a wide variety of cases, including that of weak electrolyte species. In the Supporting Information, we describe a strategy of choosing electrolytes for the case of weakly acidic species and present an example simulation of preconcentration and separation of two amino acids using bidirectional ITP.

For the case of strongly ionized analytes, we choose a high fully ionized mobility (absolute mobility), weak base for the LE+ and stronger base with low mobility for TE+. This creates a pH gradient across the initial LE+/TE+ shock, with a higher pH on the cationic TE+ side. For the anionic ITP component, we choose from relatively strong acids for LE−. We then choose a weaker acid for TE−, but one that has a high, fully ionized mobility. The latter is the key choice because we will use bidirectional ITP to effect a titration of the TE− (weak acid) to create TE− ions that overtake analyte ions after the shock interaction. After the shock interaction, TE+ (cation of strong base) replaces LE+ (cation of weak base) as the counterion for anionic ITP. This increases the local pH of anionic ITP zones and therefore raises the local value of effective mobility of TE− ions.

In contrast, the effective mobilities of LE− ions and the anionic analytes do not change appreciably after the shock interaction because they are anions of relatively stronger acids. If we make these choices correctly, the shock interaction causes the effective mobility of TE− to increase to a value larger than that of analyte ions. This then violates the ITP focusing condition given by eq 1 and initiates electrophoretic separation.

This transition from focusing to separation is analogous in function to t-ITP.[20−22] However, in t-ITP, LE ions are injected behind the focused analytes (typically by deactivating applied current and effecting a buffer exchange at the TE reservoir[22]) to initiate electrophoretic separation. Here, we use the titration caused by the interaction between cationic and anionic ITP shocks to effect a change in the mobility of TE ions such that they themselves overtake the focused analytes. Our method therefore features an initial condition that governs both focusing and separation dynamics, and the transition from ITP to separation can be initiated automatically with no buffer exchange or intermediate injections. As we show below, our method also achieves this transition with much less dispersion of the focused analytes compared with that in t-ITP.

We here provide specific examples of viable electrolyte chemistries for our method. Note that a key requirement is that the

Table 1. Possible Cationic Buffer Systems for Coupled Preconcentration and Separation of Anions Using Bidirectional ITP

|	$\mu_{+1} (\times 10^{-9} \text{ m}^2 \text{ V}^{-1} \text{ S}^{1-})$	$pK_{a,1+}$
Cationic LE (LE+)		
imidazole	52	7.15
3-methyl pyridine	40.1	5.2
4-methyl pyridine	40.1	6.2
Cationic TE (TE+)		
arginine[a]	26.9	8.92
Tris	29.5	8.08
amediol	33.5	8.78

[a] Arginine has two other ionization states corresponding to $pK_{a,1−}$ = 12.48 and $pK_{a,2+}$ = 1.78. However, Arginine is primarily disassociated in its 1+ state under safe pH[10] conditions of 5 < pH < 9.

LE+ should be a cation of a weak base with high fully ionized mobility, and TE+ should be a cation of a strong base with low fully ionized mobility. For strong base, fast cations, we can use Na$^+$ and K$^+$. However, several choices exist for high fully ionized mobility cations of weak bases and low fully ionized mobility cations of strong bases. Table 1 shows three choices each for cationic LE and TE (nine usable combinations of LE+ and TE+) that satisfy our requirements.

Another requirement is that the effective mobility of TE− ions should be less than that of analyte ions when the buffering counterion is LE+ and otherwise when the counterion is TE+. To effect a substantial increase in effective mobility of TE− after the shock interaction, TE− should therefore be a weak acid such that $pK_{a,LE+} < pK_{a,TE−} < pK_{a,TE+}$. For example, in our experiments, we used tricine ($pK_{a,TE−}$ = 8.15) as TE− along with imidazole ($pK_{a,LE+}$ = 7.15) as LE+ and arginine ($pK_{a,TE+}$ = 8.92) as TE+. On the other hand, there are no specific constraints on LE−, which can be any fast ion, such as Cl$^−$ and SO$_4^{2−}$.

We note that our bidirectional ITP experiments are compatible with both "semi-infinite" and "finite" sample injection schemes. For example, in Figure 1a, we show a semi-infinite sample injection scheme wherein sample ions are initially mixed in the LE−/LE+ mixture. Such an injection scheme both increases sensitivity (by continuously focusing sample until the shock interaction) and minimizes the complexity of the injection protocol. Alternatively, semi-infinite sample injection can be performed by mixing the sample ions in the TE−/LE+ reservoir. As a third alternative, sample ions can be injected using a more traditional finite injection protocol wherein a finite amount of analyte mixture is initially sandwiched between pure LE−/LE+ and TE−/LE+ zones. However, we emphasize that the choice of sample injection scheme does not have a significant effect on the transition from ITP to CE mode or the quality of CE separation.

Simulations of Bidirectional ITP for both Focusing and Separation of Analytes. We performed simulations of coupled ITP focusing and electrophoretic separation of two model analytes in bidirectional ITP using the SPRESSO simulation tool.[25,28,29] For our simulations, we used 75 mM HCl as LE−, 20 mM tricine as TE−, 150 mM imidazole as LE+, and 30 mM arginine as TE+. To illustrate the technique, we used two model anionic analytes, S1− and S2−, for the simulation with mobilities −20 × 10^{-9} m^{2}V^{-1}s^{-1} and −12 × 10^{-9} m^{2}V^{-1}s^{-1}, respectively. These analytes were assumed to be fully ionized under the
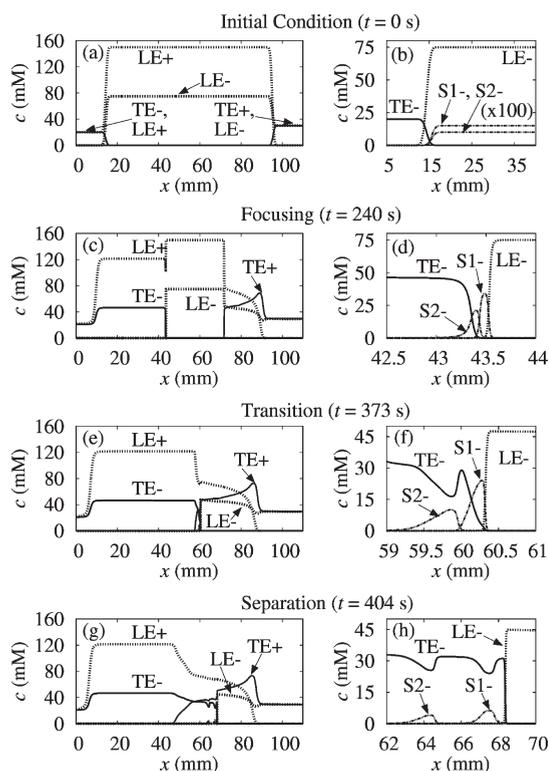
Figure 2. Simulation showing focusing and separation of species using bidirectional ITP. Plots in second column are detailed views of the distributions in the first column. (a, b) Initial distribution of chemical species in the separation channel prior to activating current. (c, d) LE−/TE− and LE+/TE+ shocks after the electric field is applied. (c) shows LE−/TE− shock ($x = 43$ mm) propagating rightward and a LE+/TE+ shock ($x = 70$ mm) propagating leftward. (d) shows anionic analytes S1− and S2− focused between LE− and TE−. (e, f) Transition from focusing to separation upon the interaction of LE−/TE− and LE+/TE+ ITP shocks. The high pH TE+ zone washes over the focused anionic analytes, increasing the effective mobility of TE− ions, but only negligibly affecting the mobility of S1− and S2−, which are stronger acids. Here, the effective mobility of TE− increases above those of S1− and S2−, thereby initiating separation. (f) TE− overtaking focused S1− and S2−, thus initiating electrophoretic separation. (g, h) Final state, in which analytes S1− and S2− are fully separated. (g) Anionic ITP shock at $x = 68$ mm and an expansion wave ($x = 50$ mm) due to disrupted cationic ITP. (h) Fully separated peaks of S1− and S2−, but an intact ITP interface between LE− and TE−. Simulations were performed using our open source code Spresso.[28,29] Chemistry is described in text. We assumed a constant current of 1.4 μA and a D-shaped, wet-etched channel 74 μm wide and 12 μm deep. We approximately account for electroosmotic flow using a constant and uniform electroosmotic mobility of 2×10^{-9} m^{2}V^{-1}s^{-1}.

conditions of simulation. Figure 2a,b shows the initial conditions of the simulation.

Analytes S1− and S2− were initially mixed in the LE−/LE+ mixture at concentrations of 15 and 10 μM, respectively. When an electric field is applied, LE−/TE− and LE+/TE+ shocks propagate toward the right and the left, respectively. Prior to shock interaction, analytes S1− and S2− focus between the LE− and TE− ions, as shown in Figure 2d. For this particular buffer chemistry, LE+ and TE+ form a shared cationic ITP zone, as shown in Figure 2c. (We see a shared zone since the effective mobility of LE+ ions in the TE+ zone is smaller than that of TE+ ions, but the effective mobility of LE+ ions in the LE+ zone

is greater than that of TE+ ions.) When the LE+/TE+ and LE−/TE− shocks interact (Figure 2e,f) the effective mobility of TE− increases, and it overtakes the focused analytes S1− and S2−. This initiates electrophoretic separation of S1− and S2−.

Figures 2g,h shows the final state when both analyte ions, S1− and S2−, are fully separated. We note that for electrophoretic separation to occur, it is necessary for TE− ions to overtake the focused analytes. However, TE− ions need not overtake LE− ions, and the LE−/TE− shock may persist, as shown in Figures 2g,h. In contrast, the shock interaction interrupts the LE+/TE+ interface, and this interface mixes (via electromigration dispersion) thereafter. That is, after the shock interaction, TE− replaces LE− as the counterion for cationic ITP. Since the conjugate acid of TE− is weaker than the conjugate acid of LE−, the pH of cationic ITP zones increases after the shock interaction. As a result, the effective mobility of LE+ (cation of a weak base) decreases considerably compared with TE+ (cation of a strong base), causing disruption of the cationic ITP interface.

Simulation results, shown in Figure 2, highlight the advantages of focusing and separation using bidirectional ITP over t-ITP. As shown in Figures 2e, f, TE− ions begin overtaking focused analyte ions (S1− and S2−) as soon as the LE+/TE+ shock wave washes over the focused analyte ions. Thus, the transition from focusing to separation occurs quickly after shock interaction. This is in contrast with t-ITP, in which LE ions injected behind the TE zone must first overtake the entire TE zone before disrupting the ITP focusing.[20,21,30] More importantly, in t-ITP, LE ions injected behind the TE zone first tail into analyte zones and effect a longer, more gradual disruption of ITP focusing.[22] The latter can lead to significant electromigration dispersion of the analyte zones prior to separation. Here, we observe a rapid change of local electromigration conditions (from ITP to zone electrophoresis separation) during which we observe negligible dispersion. (Later in this section, we compare the separation resolution of bidirectional ITP and t-ITP using numerical simulations.) Rapid transition from ITP to CE in our technique is especially important for on-chip systems in which channel lengths may be limited. Finally, the transition from focusing to separation in bidirectional ITP is fully automated and does not require buffer replacement or switching electric field between column-coupled channels, as in t-ITP.[20] Thus, the current technique can be easily adapted for on- or off-chip single-channel systems, including commercial CE systems.

We also performed a simulation under conditions where we can directly compare numerical predictions with experimental visualization of interacting shocks waves. For this, we used the same ITP chemistry and the initial conditions as in the previous simulation (Figure 2), but instead of analytes S1− and S2−, we used a fluorescent nonfocusing tracer (NFT). The NFT does not disturb or change the ITP or focus during ITP, but its concentration adapts to the local electric fields in each ITP zone (see Figure 3a). Thus, the regions of varying fluorescence intensity highlight and denote different ITP zones (more on NFT visualization technique[27] in the Experiments section).

Figure 3a shows a simulated spatiotemporal plot of the fluorescence intensity of the fluorescent NFT in the channel during bidirectional ITP. The scalar quantity plotted here is the fluorescence intensity of NFT (averaged along the channel width) as a function of distance along the axis of the channel (abscissa) and time (ordinate). Our simulation neglects the effects of photobleaching, and we assume a linear relationship between fluorescence intensity and the NFT concentration.
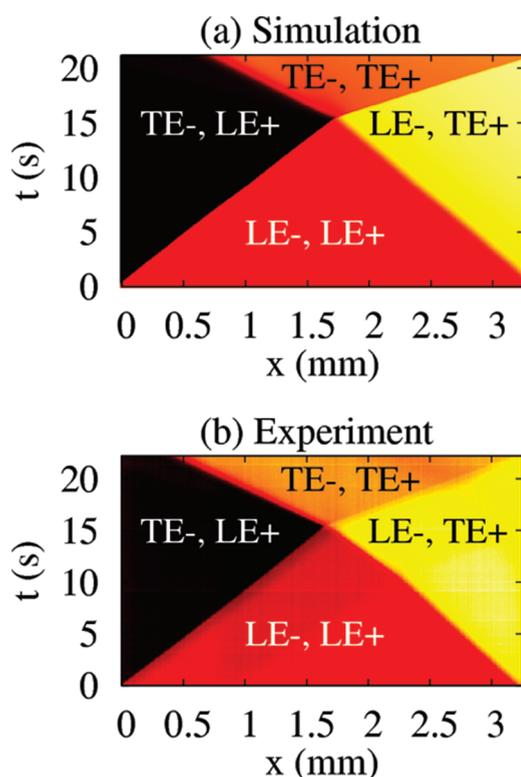
Figure 3. Numerical simulation and experimental visualization of interacting anionic and cationic ITP shocks. (a) Numerical simulation of propagating LE−/TE− and LE+/TE+ shocks. The spatiotemporal plot shows the intensity of a fluorescent nonfocusing tracer (NFT)[27] versus distance along the channel axis, x, and time, t. The NFT does not focus via ITP, but its concentration adapts to the local electric field in each zone. Regions of different fluorescence intensity mark ITP zones. (b) Experimental visualization of the same process using the fluorescent nonfocusing tracer (NFT) technique.[27] Both parts show LE−/TE− and LE+/TE+ shocks propagating toward the right and left, respectively. These shocks meet near x = 1.6 mm. The rightward-traveling LE−/TE− shock remains intact (positive slope to the right of x = 1.6 mm). In contrast, the LE+/TE+ interface is disrupted, and the interface starts to mix (barely noticeable in this field of view). To account for electroosmotic flow in our simulation, we used a constant electroosmotic mobility of $2 \times 10^{-9} \, \text{m}^2 \, \text{V}^{-1} \, \text{s}^{-1}$. We used Rhodamine 6G as the NFT. We applied a $1.4 \, \mu\text{A}$ current across a D-shaped, wet-etched, $74 \, \mu\text{m}$ wide and $12 \, \mu\text{m}$ deep channel.

The plot shows an anionic ITP (LE−/TE−) shock and a cationic ITP (LE+/TE+) shock propagating toward the right and the left, respectively. After these shock waves meet, the rightward traveling LE−/TE− shock remains intact because LE− ions (Cl⁻) have higher effective mobility than TE− ions (tricine), even after the shock interaction. On the other hand, shock interaction disrupts the leftward propagating LE+/TE+ shock, creating a rarefaction wave (the zones gradually mix via electromigration dispersion). In this simulation, we used a constant electroosmotic mobility of $2 \times 10^{-9} \, \text{m}^2 \, \text{V}^{-1} \, \text{s}^{-1}$ as our only fitting parameter to match all experimentally measured wave speeds (see Experiments section).

Comparison of Bidirectional and Transient ITP. We here compare traditional unidirectional t-ITP and bidirectional ITP using numerical simulations. Parts (a) and (b) of Figure 4, respectively, show simulated spatiotemporal plots of these two cases. In both cases, we consider the same anionic analytes (S1− and S2−)
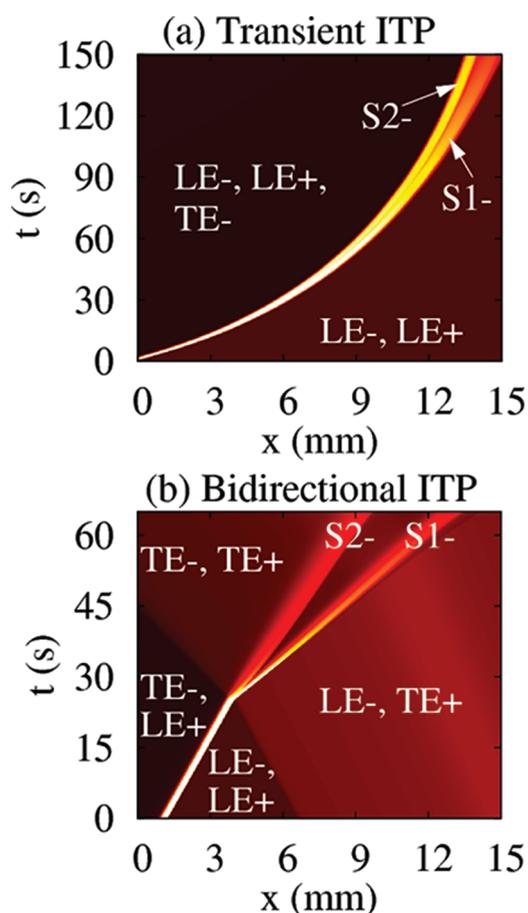
Figure 4. Simulations comparing unidirectional transient ITP (t-ITP) and bidirectional ITP. (a, b) Simulated spatiotemporal diagrams of focusing and separation of two anionic species (S1− and S2−) in t-ITP and bidirectional ITP, respectively. Both plots show fluorescence intensity of S1−, S2− and a nonfocusing tracer (NFT)[27] versus distance along the channel axis, x, and time, t. Background fluorescence values correspond to NFT concentration in various ITP zones. The brighter zones correspond to the analyte peaks. (a) t-ITP process in which S1− and S2− are initially (t < 25 s) focused in a narrow zone. This focused ITP zone propagates toward the right until it is disrupted by the overtaking LE− ions. Around t = 25 s, ITP focusing is disrupted, and the S1− and S2− zones start separating. This transition is gradual and yields significant electromigration dispersion. (b) S1− and S2− ions initially (t < 25 s) focused at the LE−/TE− interface of bidirectional ITP. The LE−/TE− shock propagates rightward (positive slope for t < 25 s), and the LE+/TE+ shock propagates leftward. These shocks interact near x = 4 mm at t = 25 s and very quickly initiate electrophoretic separation of S1− and S2−. This fast ITP-to-CE transition results in much less electromigration dispersion, higher separation resolution, and smaller analysis time. The chemistry used here is described in the text. The channel dimensions, applied current, and EOF mobility were the same as those used for Figure 2.

as in Figure 2, but to aid in visualization of various ITP zones, we also consider addition of a NFT that is initially mixed with LE−/LE+ buffer. The background fluorescence intensity values in Figures 4a, b therefore correspond to the concentration of NFT in the various ITP zones, and the brighter zones correspond to the analyte peaks.

For the anionic t-ITP simulations, we used the anionic ITP chemistry (with LE+ as the counterion), channel geometry, and

applied current of the simulation of Figure 2. Traditional anionic t-ITP does not involve cationic ITP, so we did not use TE+ in the t-ITP simulations. We first performed simulation of ITP focusing of analyte ions, S1− and S2−, between zones of LE− and TE− ions. We then stopped the simulation and replaced TE− ions in the TE−/LE+ reservoir (near the leftmost boundary) with LE− ions; this initiated the process of disrupting ITP. Figure 4a shows S1− and S2− ions initially focused in a narrow ITP zone that propagates rightward at a constant speed (the constant slope line for $t < 25$). Around $t = 25$ s and $x = 4$ mm, LE− ions begin overtaking the focused analytes and initiate electrophoretic separation of S1− and S2−. Figure 4a shows the separation phase of t-ITP for $t > 25$ s, during which the distance between the analyte peaks increases over time while the peaks themselves broaden due to diffusion and electromigration dispersion. Interestingly, during the transition from ITP focusing to CE separation, the speed of the analyte zones decreases considerably. This deceleration of analyte zones is apparent in Figure 4a, where the analyte peak locations vary nonlinearly with time after $t = 25$ s. A similar deceleration of analyte zones in t-ITP has been observed experimentally by Chambers and Santiago.[27] The transition phase in t-ITP is slow, analytes zones disperse, and the distance between the analyte peaks does not exceed their characteristic widths until about $t = 90$ s.

For the bidirectional ITP simulation (Figure 4b), we used the same conditions as those of Figure 2, including the electrolyte chemistry, applied current, and the channel geometry; the only difference being the presence of NFT in Figure 4b. We note that the results shown in Figures 2 and 4b are quite similar, because the presence of the NFT in trace amounts ($100\,\mu$M initial concentration) has a negligible effect on local electric fields and focusing and separation of S1− and S2−. Figure 4b shows the LE−/TE− shock wave propagating toward the right and the LE+/TE+ shock wave propagating toward the left (for $t < 25$ s). Analytes S1− and S2− initially focus at the LE−/TE− interface. When the LE−/TE− and LE+/TE+ shock waves interact around $x = 4$ mm and $t = 25$ s, ITP focusing of S1− and S2− very quickly transitions to CE separation. Thereafter (for $t > 25$ s), the relative distance between S1− and S2− peaks keeps increasing while the peaks gradually diffuse over time.

Comparison of Figures 4a and b show that the analyte peaks in bidirectional ITP are much better resolved than in t-ITP. That is, for the same distance between the two peaks, the peaks in bidirectional ITP are much less dispersed than in t-ITP. Bidirectional ITP yields higher resolution separations, since the ITP-to-CE transition in bidirectional ITP occurs quickly after the anionic and cationic ITP shocks interact. Thus, analytes are exposed to local conductivity gradients (which cause electromigration dispersion) for a much shorter distance and time. In contrast, in t-ITP, LE− ions injected behind the TE− zone tail significantly into the focused analyte zones and only gradually and slowly disrupt ITP preconcentration,[22] yielding significant and prolonged electromigration dispersion. In addition to better resolution, the faster ITP-to-CE transition offered by bidirectional ITP results in reduced separation time and an increased signal-to-noise ratio for a given resolution. Compare, for example, the resolution obtained by bidirectional ITP in Figure 4b at $t = 45$ s. Such resolution is not observed in the t-ITP case (Figure 4a), even at $t = 150$ s. In the Supporting Information, we show a plot of resolution vs time for both bidirectional ITP and t-ITP using the simulation data of Figures 4a,b.

■ MATERIALS AND METHODS

We performed experiments to visualize interacting cationic and anionic ITP shock waves in bidirectional ITP using the NFT technique[27] (cf. the Experiments section). For these visualization experiments, LE− was the chloride ion from 75 mM HCl, TE− was 20 mM tricine, LE+ was 150 mM imidazole, and TE+ was 30 mM arginine. We prepared 10 mM stock solution of the Rhodamine-6G dye (Invitrogen, Carlsbad, CA) and used it as an NFT by mixing at a concentration of $100\,\mu$M in the LE+/LE− mixture.

For the experiments demonstrating coupled ITP preconcentration and separation of DNA fragments, we used the chloride ion from 150 mM HCl as LE−, 20 mM tricine as TE−, 300 mM imidazole as LE+, and 30 mM arginine as TE+. We added a 1 kbp DNA ladder from New England BioLabs (Ipswich, MA) to the mixture of LE+ and LE−, with a final concentration of 50 ng/mL. We used 0.75% w/w hydroxyl ethyl cellulose (HEC) as a sieving matrix (mixed with LE−) to achieve a size dependence on the mobility of fragments, because the free solution mobility of ds-DNA fragments greater than ∼400 bp is effectively independent of molecular weight.[31] To visualize the DNA fragments, we used the fluorescent intercalating dye SYBR Green I (Invitrogen, Carlsbad, CA). (We note that intercalating dyes, such as SYBR Green I, should be handled carefully due to their potential mutagenic properties.[32])

We prepared 1 M stock solutions of HCl, tricine, and imidazole and 300 mM stock solution of arginine hydrochloride before diluting them to the desired concentrations in different solutions. We added 1% w/w polyvinylpyrrolidone (PVP) to all solutions to suppress electroosmotic flow. All chemicals were obtained from Sigma Aldrich (St. Louis, MO) and were prepared in UltraPure DNase/RNase-free distilled water (GIBCO Invitrogen, Carlsbad, CA).

We captured images using an inverted epifluorescent microscope (IX70, Olympus, Hauppauge, NY) equipped with a LED lamp (LEDC1, ThorLabs, Newton, NJ), U-MWIBA filter cube from Olympus (460−490 nm excitation, 515 nm emission, and 505 nm cutoff dichroic) and a 10× (NA = 0.3) UPlanApo objective (Olympus, Hauppauge, NY). Images were captured using a 12 bit, 1300 × 1030 pixel array CCD camera (Micromax1300, Princeton Instruments, Trenton NJ). We controlled the camera using Winview32 (Princeton Instruments, Trenton NJ) and processed the images with MATLAB (R2007b, Mathworks, Natwick, MA). We conducted the experiments by applying either constant voltage or current using a sourcemeter (model 2410, Keithley Instruments, Cleveland, OH).

For all our experiments, we used off-the-shelf Caliper NS-95 borosilicate glass microchips from Caliper Life Sciences (Mountain View, CA). Figure 5a shows a schematic of the channels with cross-geometry. The channels consist of a wider loading section (50 μm mask width) and a narrower separation section (10 μm mask width). All channels are wet-etched to a depth of 12 μm. The variable cross-sectional geometry allows us to achieve higher sensitivity in ITP by focusing a large amount of sample in the loading section prior to entering the separation channel.[33,34]

■ EXPERIMENTS

We first performed on-chip bidirectional ITP experiments to visualize interacting cationic and anionic ITP shock waves. For these experiments, we did not focus analytes, but instead, visualized the interaction of cationic and anionic LE/TE interfaces.

We used these visualization experiments to optimize our injection protocol to precisely control the location of shock interaction. We then performed bidirectional ITP experiments to demonstrate coupled preconcentration and high-resolution separation of DNA fragments from a 1 kbp ds-DNA ladder.

Visualization of Interacting Shocks in Bidirectional ITP. We visualized interacting anionic and cationic ITP shocks in bidirectional ITP using the NFT technique.[27] In the NFT technique, fluorescent, co-ionic species that do not obey the ITP focusing conditions given by eqs 1 and 2 are mixed with the ITP buffers. These fluorescent species do not focus, but their concentration adapts to a local electric field in different ITP zones to maintain the continuity of electromigration flux. For our experiments, we used a 100 μM concentration of Rhodamine-6G (R6G, a cationic dye) in the LE+/LE− mixture as the NFT. In our experiments, R6G is slower than the cationic TE ions and so does not focus. Hence, we visualized propagating anionic and cationic ITP shock waves simultaneously using a single nonfocusing fluorescent species (Rhodamine-6G). The experimental protocol for these experiments is discussed in the Supporting Information.

Figure 3b shows an experimentally measured spatiotemporal plot of fluorescence intensity in a bidirectional ITP experiment with converging shock waves. To obtain this spatiotemporal plot, we captured CCD camera images of fluorescence intensity in a 3.25 mm long section of the channel at a rate of 10 frames/s. We then width-averaged the fluorescent intensity for 210 images and plotted this axial intensity distribution for each point (in time) along the ordinate. In Figure 3b, the abscissa is the axial distance along the channel, the ordinate is time, and the intensity of the plotted scalar is the measured fluorescence intensity. The slopes of features in such spatiotemporal plots are therefore inversely proportional to the velocities of ITP zone interfaces. Figure 3b shows that, prior to the shock interaction ($t < 15$ s), the LE−/TE− shock propagates toward the right, and the LE+/TE+ shock, toward the left. After the LE−/TE− and LE+/TE+ shocks interact (at $x = 1.6$ mm and $t = 15$ s), the LE+/TE+ interface is disrupted, and a rarefaction wave ensues. This is because the effective mobility of TE+ becomes higher than LE+ after the shock interaction. However, after the shock interaction ($t > 15$ s), the LE−/TE− interface remains intact because the mobility of fully ionized chloride ion (LE−) remains higher than the effective mobility of tricine (TE−) throughout the experiment. Our experimental visualization results compare well with the simulated spatiotemporal diagram shown in Figure 3a. Our simulations correctly predict the persistence of LE−/TE− interface and the disruption of the LE+/TE+ interface after the shock interaction. We use an electroosmotic mobility value of 2×10^{-9} m^2 V^{-1} s^{-1} as the only fitting parameter, and yet, the simulations correctly predict the time and the location of shock interaction and the four observable propagation velocities.

We note that experimental visualization and simulations of interacting shocks in bidirectional ITP are particularly helpful in tuning the initial conditions to precisely select the location of shock interaction and transition from ITP focusing to electrophoretic separation. For our experiments on DNA separations, we used a NFT[27] to tune our injection protocol to initiate electrophoretic separation as soon as the focused analytes entered the narrow separation channel. This allowed us to obtain higher resolution by using the entirety of the separation channel for the CE mode.
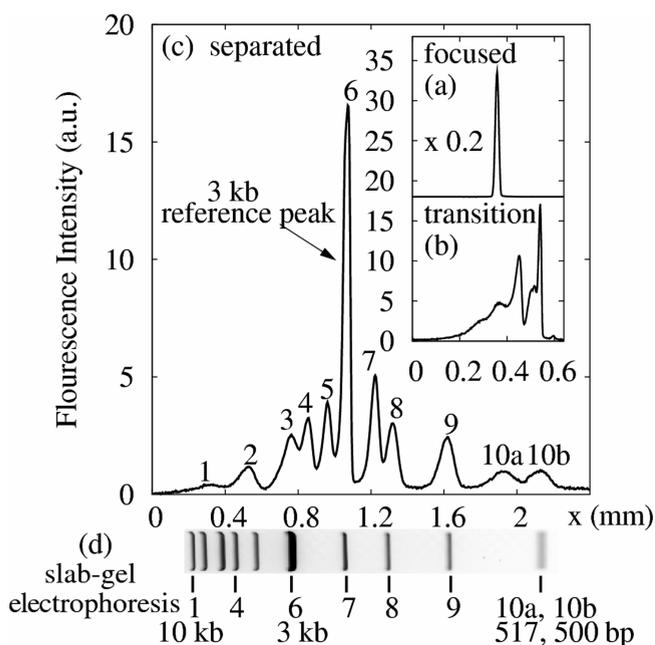
Coupled Preconcentration and Separation of DNA Fragments. We performed experiments to demonstrate coupled ITP
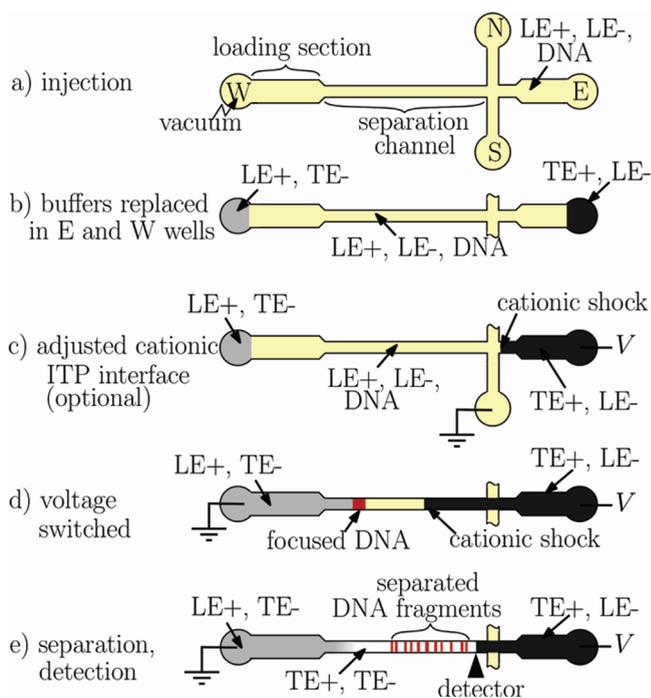
Figure 5. Protocol for DNA separations using bidirectional ITP leveraging channel cross-sectional area reduction for increased sensitivity. For DNA separation experiments, (a) we injected the mixture of LE+, LE− and DNA fragments by applying a vacuum on the W well. We then emptied the E and W wells and (b) filled the E and W wells with a TE+/LE− mixture and a LE+/TE− mixture, respectively. (c) We then moved the LE+/TE+ interface up to the junction by applying voltage between the E and S wells. We performed this optional step to ensure that the LE−/TE− and LE+/TE+ shocks interacted precisely near the entrance of the separation channel (the smaller cross section channel). (d) We then switched the electrodes between the E and W wells. The LE+/TE+ shock meets the focused DNA fragments and initiates electrophoretic separation. (e) We imaged the separated DNA fragments at the end of the separation channel. No manual buffer exchanges are needed once the voltage is applied, and we stress that the voltage switching used here is optional.

preconcentration and electrophoretic separation of DNA fragments using bidirectional ITP. The injection protocol for these experiments is shown in Figure 5. Briefly, we first filled all channels with a mixture of LE+, LE−, and DNA fragments. We then emptied the east and the west wells and filled them with a TE+/LE− mixture and a LE+/TE− mixture, respectively. We then moved the LE+/TE+ interface up to the junction by applying voltage across the east and south wells. This optional step ensured that the LE+/TE+ shock interacted with focused anions earlier in the narrow separation channel. We then applied voltage across the wast and the east wells and visualized separated DNA fragments at the end of separation channel. (We note that caution should be taken, and the high voltage supply should be turned off while manually switching electrodes, as shown in Figure 5.)

As shown in Figure 5d, prior to the shock interaction, the 1 kbp ds-DNA ladder is focused between the LE− and the TE− zones. When the LE+/TE+ shock washes over the focused DNA fragments, both the pH of the TE− zone and the effective mobility of TE− ions increase. However, under the conditions of our experiments (pH > 7), DNA fragments are fully ionized, and

Figure 6. Experimental preconcentration and separation of 1 kb ds-DNA ladder using bidirectional ITP. (a) Initially focused DNA fragments in anionic ITP. (b) Transition from focusing to separation after the cationic ITP interface washes over the focused DNA fragments. (c) Fully resolved DNA ladder with 11 peaks at the end of separation channel. (d) Visualization (inverted) of agarose gel electrophoresis separation (provided by the vendor, New England BioLabs, Ipswich, MA). Note that the agarose gel does not resolve peaks 10a and 10b corresponding to 517 and 500 bp fragments. The electropherogram at (c) is measured 15 mm to the right of the point where the shocks interact. For this experiment, we used a semi-infinite injection of DNA sample to increase the detection sensitivity and minimize the injection complexity.

any increase in pH has no significant effect on the effective mobility of DNA fragments. TE− ions, therefore, overtake focused DNA after the shock interaction, initiating electrophoretic separation in the HEC sieving matrix (shown schematically in Figure 5e). In our experiments, we used a semi-infinite injection scheme by mixing DNA fragments with the LE− and LE+ mixture to increase the sensitivity by continuously focusing DNA fragments until the shock interaction. We note that the DNA fragments can also be initially mixed with LE+/TE− mixture.

Figure 6 shows the results of DNA preconcentration and separation using bidirectional ITP. Initially, all DNA fragments are focused in a thin zone between the LE− and TE− zones (Figure 6a). Later, the shock interaction initiates CE separation of focused DNA fragments. The initial phase of CE separation is shown in Figure 6b. Figure 6c shows an electropherogram measured at the end of separation channel showing a fully resolved DNA ladder consisting of distinct peaks 1−11 corresponding to the 10, 8, 6, 5, 4, 3, 2, 1.5, 1, 0.517, and 0.500 kbp fragments. The electropherogram from our experiments is in qualitative agreement with slab gel separations of the same DNA ladder (provided by the vendor, New England BioLabs, Ipswich, MA). We note that peaks 10a and 10b (corresponding to 500 and 517 bp) are clearly resolved by our technique (see Figure 6c) but not resolved in agarose gel electrophoresis (e.g., Figure 6d). These distinct peaks corresponding to 500 and 517 bp have also been observed for this ladder in higher resolution separations on polyacrylamide gels.[35] For these

experiments, we diluted the DNA to 50 ng/mL concentration in the LE+/LE− mixture with only 1 pg of DNA initially injected into the separation channel.

■ CONCLUSIONS

We have developed a new technique to automatically couple isotachophoretic preconcentration and electrophoretic separation via shock interaction in bidirectional ITP. We have described how interaction of cationic and anionic ITP shocks in converging bidirectional ITP can lead to fundamental changes in focusing behavior of analytes. We leveraged shock interaction in bidirectional ITP to precisely change the pH of migrating zones so that initially focused analytes initiate electrophoretic separation upon shock interaction. To the best of our knowledge, this is the first time that shock interaction in bidirectional ITP has been leveraged to couple different electrophoresis modes.

We discussed practical choices of electrolyte chemistries for bidirectional ITP that give electrophoretic separation after the interaction of cationic and anionic ITP shocks. To illustrate the technique and verify our choice of buffer chemistry, we performed numerical simulations using 1-D area-averaged electro-migration-diffusion transport equations. On the basis of these simulations, we showed that the transition from focusing to separation in bidirectional ITP is fast and results in negligible electromigration dispersion of electrophoretic zones. We confirmed the simulation results with indirect fluorescence visualization experiments of bidirectional ITP zones. Using a single fitting parameter (electroosmotic mobility), we showed that our simulations accurately capture the observed dynamics of shock interaction, including shock velocities and disruption of ITP interfaces after shock interaction. We then used simulations to compare separation resolution of bidirectional ITP and unidirectional t-ITP. Our simulations show that bidirectional ITP yields separations with significantly higher resolution and shorter analysis time compared with t-ITP. Finally, as an example application, we used bidirectional ITP to couple ITP preconcentration and high-resolution electrophoretic separation of DNA fragments of a 1 kbp DNA ladder. We fully resolve the ladder in 7 min (only 3 min after shock interaction) starting from a 30 μL sample dispensed into the chip reservoir at 50 ng/mL concentration (after which ~1 pg of DNA was injected into the channel) and using no manual steps.

Shock interaction in bidirectional ITP is an elegant way to couple ITP preconcentration and electrophoretic separation. The method eliminates the need for intermediate steps, such as buffer exchange and deactivation and reactivation of a power supply. Unlike t-ITP, the transition from focusing to separation in bidirectional ITP occurs over a relatively small distance (here, on the order of 1 mm), allowing optimal use of the channel length for the ITP focusing and electrophoretic separation phases. This aspect is particularly important for on-chip systems that have constraints on maximum channel length. The technique can also be applied to conventional single-channel CE systems (e.g., using fused-silica capillaries) and eliminates the need for column-coupled channels for buffer replacement.

■ ASSOCIATED CONTENT

ⓢ Supporting Information. Additional information as noted in text. This material is available free of charge via the Internet at http://pubs.acs.org.

■ AUTHOR INFORMATION

Corresponding Author

*Address: 440 Escondido Mall Bldg. 530, room 225, Stanford, CA 94305. Phone: 650-723-5689. Fax 650 723-7657. E-mail: juan.santiago@stanford.edu.

■ REFERENCES

(1) Everaerts, F. M.; Beckers, J. L.; Verheggen, Th. P. E. M. *Isotachophoresis—Theory, Instrumentation and Applications*; Elsevier: Amsterdam, 1976.

(2) Bocek, P. *Top. Curr. Chem.* **1981**, *95*, 131–178.

(3) Zhukov, M. Yu. *U.S.S.R. Comput. Math. Math. Phys.* **1984**, *24*, 138–149.

(4) Moore, G. T. *J. Chromatogr.* **1975**, *106*, 1–16.

(5) We note that "shock wave" is a generic term that has been used in the literature to describe discontinuities due to nonlinear advection flux in a variety of physical processes, such as fluid flow,[6] chromatography,[7] ITP,[3,4] sedimentation boundaries,[8] and automotive traffic flow.[9]

(6) Leveque, R. J. *Finite Volume Methods for Hyperbolic Problems*; Cambridge University Press: Cambridge, U.K., 2004.

(7) Rhee, H.-K.; Aris, R.; Amundson, N. R. *Philos. Trans. R. Soc. A* **1970**, *267*, 419–455.

(8) Probstein, R. F. *Physicochemical Hydrodynamics: An Introduction*; Wiley-Interscience: New York, 1994; Chapter 5.

(9) Richards, P. I. *Oper. Res.* **1956**, *4*, 42–51.

(10) Ermakov, S. V.; Zhukov, M. Y.; Capelli, L.; Righetti, P. G. *Electrophoresis* **1998**, *19*, 192–205.

(11) Thormann, W. *Electrophoresis* **1983**, *4*, 383–390.

(12) Thormann, W.; Arn, D.; Schumacher, E. *Electrophoresis* **1985**, *6*, 10–18.

(13) Oshurkova, O. V.; Gorshkov, A. I. *Russ. Chem. Rev.* **1993**, *62*, 729–742.

(14) Oshurkova, O. V.; Gorshkov, A. I.; Nesterov, V. P. *Russ. J. Electrochem.* **2004**, *40*, 516–520.

(15) Kohlrausch, F. *Ann. Phys. Chem.* **1897**, *62*, 209–239.

(16) Hirokawa, T.; Watanabe, K.; Yokota, Y.; Kiso, Y. *J. Chromatogr.* **1993**, *633*, 251–259.

(17) Prest, J. E.; Baldock, S. J.; Fielden, P. R.; Goddard, N. J.; Treves Brown, B. J. *Analyst* **2002**, *127*, 1413–1419.

(18) Oshurkova, O. V.; Ivanova, I. A. *Dokl. Akad. Nauk SSSR* **1976**, *227*, 1371–1374.

(19) Oshurkova, O. V.; Ivanova, I. A. *J. Anal. Chem. USSR* **1977**, *32*, 1707–1711.

(20) Foret, F.; Szoko, E.; Karger, B. L. *J. Chromatogr.* **1992**, *608*, 3–12.

(21) Foret, F.; Szoko, E.; Karger, B. L. *Electrophoresis* **1993**, *14*, 417–528.

(22) Krivankova, L.; Pantuckova, P.; Bocek, P. *J. Chromatog., A* **1999**, *838*, 55–70.

(23) Gebauer, P.; Bocek, P. *J. Chromatogr.* **1983**, *267*, 49–65.

(24) Persat, A.; Suss, M. E.; Santiago, J. G. *Lab Chip* **2009**, *9*, 2454–2469.

(25) Bahga, S. S.; Bercovici, M.; Santiago, J. G. *Electrophoresis* **2010**, *31*, 910–919.

(26) Porras, S. P.; Riekkola, M.; Kenndler, E. *Electrophoreis* **2003**, *24*, 1485–1498.

(27) Chambers, R. D.; Santiago, J. G. *Anal. Chem.* **2009**, *81*, 3022–3028.

(28) Bercovici, M.; Lele, S. K.; Santiago, J. G. *J. Chromatogr., A* **2009**, *1216*, 1008–1018.

(29) Bercovici, M.; Lele, S. K.; Santiago, J. G. *J. Chromatogr., A* **2010**, *1217*, 588–599.

(30) Xu, Z. Q.; Nishine, T.; Arai, A.; Hirokawa, T. *Electrophoresis* **2004**, *25*, 3875–3881.

(31) Stellwagen, N. C.; Stellwagen, E. *J. Chromatogr., A* **2009**, *1216*, 1917–1929.

(32) Singer, V. L.; Lawlor, T. E.; Yue, S. *Mutat. Res.* **1999**, *439*, 37–47.

(33) Dolink, V.; Deml, M.; Bocek, P. *J. Chromatogr.* **1985**, *320*, 89–97.

(34) Bahga, S. S.; Kaigala, G. V.; Bercovici, M.; Santiago, J. G. *Electrophoresis* **2011**, *32*, 563–572.

(35) New England Biolabs. http://www.neb.com/nebecomm/products/productn3232.asp.

6162

dx.doi.org/10.1021/ac200268f |*Anal. Chem.* 2011, 83, 6154–6162